PERGAMON

Deep-Sea Research II 49 (2002) 675–691

DEEP-SEA RESEARCH
PART II

www.elsevier.com/locate/dsr2

Bio-optical characteristics of Gerlache and Bransfield Strait waters during an Antarctic summer cruise

Félix L. Figueroa*

Departa ento de Ecología, Facultad de Ciencias, Universidad de Málaga, Ca pus Universitario de Teatinos s/n, E-29071 Málaga, Spain

Received 8 June 1999; accepted 6 February 2001

Abstract

Spatial and temporal variations in bio-optical characteristics of the Gerlache and Bransfield Strait waters were determined during an Antarctic summer cruise (FRUELA) in December 1995 and January 1996. Chlorophyll concentration was estimated using a bio-optical model from natural fluorescence flux over the emission of chlorophyll *a*, incident irradiance, chlorophyll specific absorption coefficient, and quantum yield of fluorescence.

The penetration of both photosynthetic active radiation (PAR) and ultraviolet radiation (UV) depended on the concentration of particulated material. Beam attenuation coefficient at 660 nm (c), a good estimator of the particulate material concentration, ranged from 0.85–2.5 m^{-1} in the upper mixed layer. The values of particulate beam attenuation and the spectral absorption coefficients suggest that the detritical contribution is relatively low and the package effect is relatively high. Both beam attenuation and vertical attenuation of downward radiation (K_d) were linearly correlated with chlorophyll concentration in the water column. Chlorophyll concentration in the study area varied two orders of magnitude (0.2–23 μg Chl $a l^{-1}$). During the cruise, the maximal UV-B incident radiation at 305 nm was variable ranging from 0.8 to 9.7 μW cm^{-2}. Great regional differences in penetration of UV-B were observed with $K_{d(305)}$ values in the upper mixed layer, ranging from 0.01 to 0.56 m^{-1}. On the other hand, the attenuation coefficient of downward PAR radiation ($K_{d(PAR)}$) in the upper mixed layer ranged from 0.08 to 0.5 m^{-1}. K_d values of both PAR and UV were higher in the stations of Gerlache Strait, coastal waters of Trinity Peninsula, and in a front system north of Bransfield. The lowest K_d values were found in Bransfield, south of King George and Livingstone islands and were associated to low cell densities and chlorophyll concentrations. The spectral light attenuation between 300 and 800 nm also was analyzed. Blue and red regions of the spectra were drastically attenuated in the surface waters of Gerlache Strait.

1. Introduction

The low rates of primary production in Antarctic waters (Smith et al., 1992; Holm-Hansen and Mitchell, 1991; Holm-Hansen et al., 1993a, b) under high nutrient concentrations have prompted to call it the major biological 'paradox' of the Southern Ocean (Weiler and Penhale, 1994). Light, temperature, trace-nutrients, grazing and mixing processes (Holm-Hansen and Mitchell, 1991), respiration (Tilzer and Dubinsky, 1987), grazing (Huntley et al., 1991), sinking (Karl et al.,

*Corresponding author. Tel.: +34-952-131672; fax: +34-952-132000.

E- ail address: felix_lopez@uma.es (F.L. Figueroa).

0967-0645/01/$ - see front matter
PII: S0967-0645(01)00118-7

Nomenclature

a_c^*	chlorophyll specific total absorption coefficient, $m^2 g^{-1}$ chl *a*
a_p^*	chlorophyll specific absorption coefficient due to particulate material, $m^2 mg^{-1}$ chl *a*
c	total beam attenuation coefficient, m^{-1}
c^*	chlorophyll specific beam attenuation coefficient, $m^2 mg^{-1}$ chl *a*
c_p	beam attenuation coefficient due particulate material, m^{-1}
c_s	beam attenuation coefficient due to dissolved material, m^{-1}
c_w	beam attenuation coefficient due to pure water by itself, m^{-1}
Chl *a*	chlorophyll, $mg\,m^{-3}$
E_o	scalar irradiance, μmol photons $m^{-2} s^{-1}$
F_f	natural fluorescence flux, nmol photons $m^{-3} s^{-1}$
Φ_f	quantum yield of fluorescence
$K_{d(\lambda)}$	spectral vertical attenuation coefficient of the downward radiation, m^{-1}
K_d^*	chlorophyll specific attenuation coefficient of the downward radiation, $m^2 mg^{-1}$ chl *a*
K_p	attenuation coefficient of the downward radiation due particulate material, m^{-1}
K_s	attenuation coefficient of the downward radiation due dissolved material, m^{-1}
K_w	attenuation coefficient of the downward radiation due clear water material, m^{-1}
L_u	upwelling irradiance over the emission of chl *a*, nmol photons $m^{-2} s^{-1} sr^{-1}$
PAR	photosynthetic active radiation ($\lambda = 400-700$ nm)
UVR	ultraviolet radiation ($\lambda = 280-400$ nm)

1991), and mean wind speed (Clarke, 1988) have all been invoked as key factors that control the phytoplankton crop.

Among these factors, solar radiation (including UV) and mixing processes have a large effect on primary production (Weiler and Penhale, 1994). The photoprotection of the photosynthetic equipment against UV radiation also has been suggested as a key factor to keep optimal rates of photosynthesis in cold waters (Vernet et al., 1994). The decrease of phytoplanktonic productivity by enhanced UV-B can be due to DNA damage (Karentz et al., 1991), a direct effect on carbon (Lesser et al., 1994; Schofield et al., 1995) and nitrogen assimilation system (Behrenfeld et al., 1995), or due to the inhibition of motility (Häder, 1994).

The depth of the mixing layer has a large influence on the photosynthetic capacity in Antarctic waters (Helbling et al., 1994). Mitchell and Holm-Hansen (1991b) evaluated the relationship between the depth of mixing, photosynthetic active radiation (PAR) and phytoplankton biomass. They found that the depth of the upper mixed layer (Z_{UML}) can be used to predict the upper limit of the phytoplankton crop size. Figueiras et al. (1994) suggested that the phytoplankton in the region is adapted to maximize its carbon uptake and growth rate at the mean irradiance of the upper mixed layer in well-mixed zones.

The main interest of the bio-optical characterization of the water column is its usefulness for the estimation of primary production. Bio-optical variables such as absorption and attenuation coefficients, quantum yield and spectral irradiance have been used in several models to estimate primary production (Lewis et al., 1985; Smith et al., 1989; Sosik, 1996).

In this study, the bio-optical characteristics of Gerlache and Bransfield Strait waters are described for both ultraviolet (UV) and PAR.

The number of studies on the light environment in Antarctica is relatively small compared to other oceans (Tilzer et al., 1994; Figueiras et al., 1994; Stambler et al., 1997). Thus, in order to explain the environmental control of primary production, it is very important to conduct studies on the underwater light field, including PAR and UV radiation (UVR), and to perform high-resolution studies on the spectral properties of the underwater light to develop bio-optical models (Prézelin et al., 1994).

2. Methods

2.1. Underwater light field

The stations at which bio-optical sampling was carried out are shown in Fig. 1. Surface UV radiation (UVR) and photosynthetic active radiation (PAR) were monitored every 2 min throughout the day with a Biospherical radiometer (PUV 510A model). Irradiances of underwater UVR and PAR were determined several times during the day by means of the PUV 500 profiling UV radiometer (Biospherical Instruments). The PUV 500 determines downwelling UV irradiance at 4 different bands: 305 ± 1 nm (band pass filter of 7 ± 1 nm), 320 ± 2 nm (band pass filter of 11 ± 1 nm), 340 ± 2 nm (band pass filter of 10 ± 1 nm) and 380 ± 2 nm (band pass filter of 10 ± 1 nm) and PAR radiation by means of a broadband PAR sensor (400–700 nm). The PUV 500 system was equipped with a pressure sensor (depth) and a Sea Tech transmissometer (25 cm path length) to determine the percentage of transmission of the water at each depth. The transmissometer was provided with a FFE-3100 LED light source with a peak wavelength at 660 nm and spectral line width of 40 nm.The total beam attenuation coefficient (c) expressed in m^{-1}, which is a good estimator of the concentration of particulated material, was calculated according to the equation

$$c = (\ln T)/z \quad \text{units}: \ m^{-1}, \tag{1}$$

where T is the transmission and z the path length of the transmissometer (0.25 m).

The total beam attenuation coefficient can be expressed as the addition of the attenuation coefficients due to pure water by itself (c_w), particulate material (c_p), and dissolved matter (c_s). However, beam attenuation in the red part of the spectrum depends mainly on the optical properties of the cell suspension (c_p), its concentration in the seawater, and the attenuation by the water itself (c_w), while the role of dissolved substances is negligible (Jerlov, 1976).

The specific beam attenuation coefficient is defined as

$$c^* = c/[\text{Chl}\,a] \quad \text{units}: \ m^2\,\text{mg Chl}\,a^{-1}. \tag{2}$$

The vertical attenuation coefficients of the downward radiation (K_d) in the four UV bands and PAR ($K_{d(305)}$, $K_{d(320)}$, $K_{d(340)}$, $K_{d(380)}$ and $K_{d(PAR)}$) were calculated by linear regression between surface (0.1 m depth) and 30 m depth following the equation

$$K_d = (\ln I_o - I_z)/z \quad \text{units}: \ m^{-1}. \tag{3}$$

I_o, being the irradiance at the surface (0.1 m depth) and I_z the irradiance at a determined depth (z).

The vertical attenuation coefficient can be expressed as the addition of the attenuation coefficients due to the clear ocean water by itself (K_w), soluble material (K_s) including dissolved organic matter and gilvinic substances, and particulate material including phytoplankton (K_d):

$$K_d = K_w + K_s + K_p \quad \text{units}: \ m^{-1}. \tag{4}$$

Specific attenuation coefficient (K_d^*) was calculated as the slope between attenuation coefficient (K_d) minus the attenuation coefficient due to clear oceanic water (K_w) and Chl a concentration. The values of K_w were taken from Smith and Baker (1978) and Morel (1988):

$$K_d - K_w = K_s + K_d^*\,\text{Chl}\,a \quad \text{units}: \ m^{-1}, \tag{5}$$

$$K_d^* = [(K_d - K_w) - K_s]/\text{Chl}\,a \quad \text{units}: \ m^2\,\text{mg Chl}\,a^{-1}. \tag{6}$$

2.2. Esti ation of Chl a concentration fro bio-optical odels

Fluorescence of chlorophyll provides an index of chlorophyll a concentration (Kishino et al., 1985). Thus natural fluorescence was determined according to Kiefer et al. (1989) using a natural fluorescence sensor (PUV-683) from Biospherical Instruments, included in the PUV-500 radiometer. The volume fluorescence flux of natural fluorescence (F_f) is the measurement of light per unit volume. It is assumed that the source (chlorophyll fluorescence) can be calculated from the measurement of upwelling radiance, specifically over the emission of chlorophyll a, and the quantum yield of natural fluorescence. Thus, the following expression is used (Kiefer

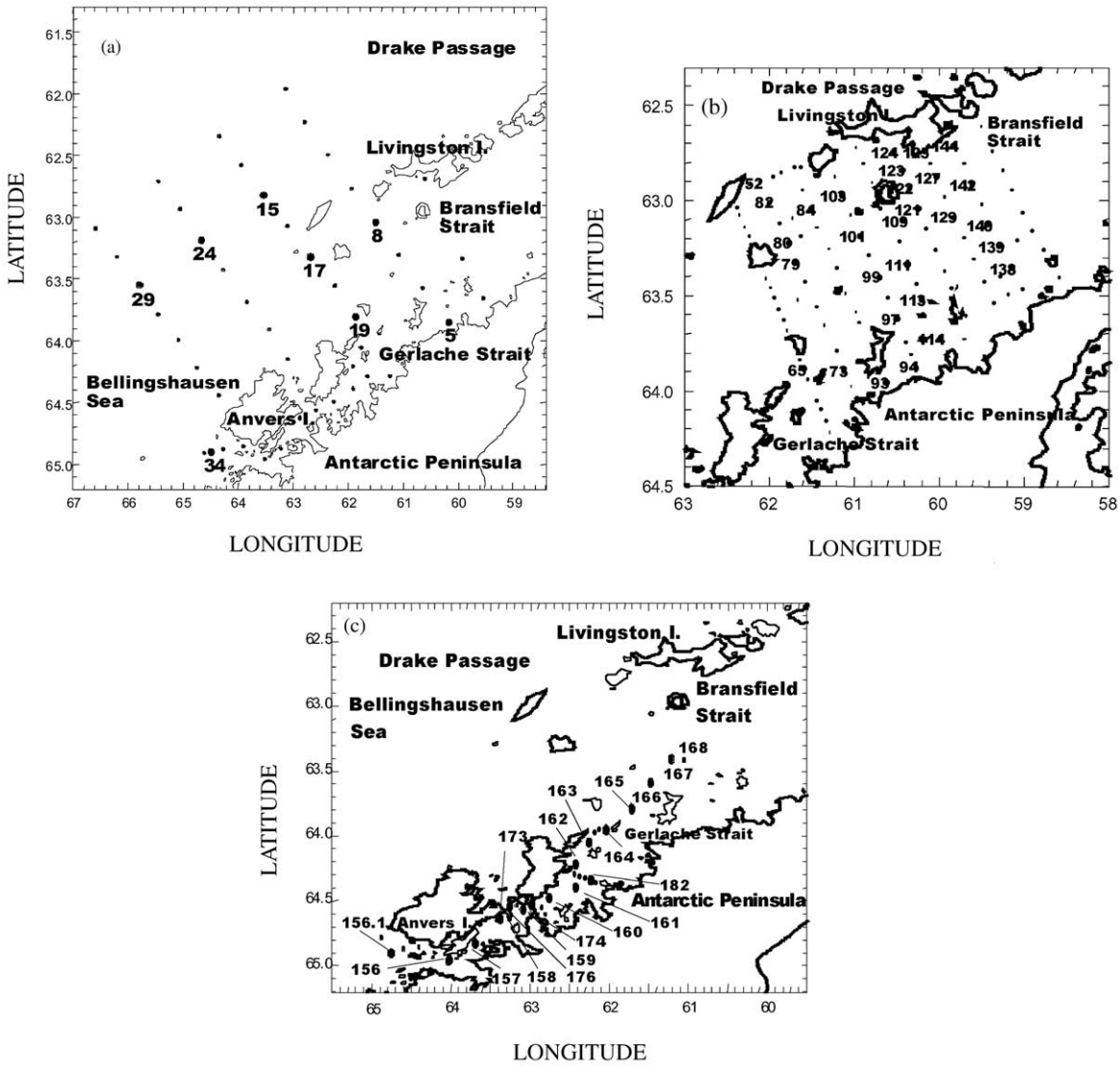

Fig. 1. Chart of the sampling area showing the positions of CTD stations. The numbered larger circles correspond to the stations where bio-optical sampling was done. The location of the three main hydrographic features is shown: Ice-Edge; WSC, Weddell Scotia Confluence; FRONT is the frontal structure that separates Bransfield waters with influence of Bellingshausen Sea (northern area) from Bransfield waters with influence of the Weddell Sea.

et al., 1989):

$$F_f = 4\pi(K_{d(PAR)} + a(\mathrm{Chl}))L_u(\mathrm{Chl})$$
$$\text{units}: \ \mathrm{nmol\,photons\,m^{-3}\,s^{-1}}. \qquad (7)$$

4π is a geometric constant with units of stereoradians (sr), $K_{d(PAR)}$ (m^{-1}) is the vertical attenuation coefficient of downward radiation for PAR calculated from the irradiance measurements, a (Chl) is an absorption coefficient for water, and L_u (Chl), $\mathrm{nE\,m^{-2}\,s^{-1}\,sr^{-1}}$, is the upwelling radiance specifically over the emission of chlorophyll a. This is valid since there is little difference between the attenuation coefficients for scalar irradiance and

cosine irradiance of PAR (Chamberlin et al., 1990). The total absorption coefficient for water (a (chl)) is weighted over the emission (not absorption) spectrum of chlorophyll. Over this region, a (chl) is most strongly influenced by water absorption and is assumed to be constant ($0.48\,m^{-1}$). These terms are used to convert the radiance measurement ($\mu mol\,m^{-2}\,s^{-1}\,sr^{-1}$) to volume fluorescence ($\mu mol\,m^{-3}\,s^{-1}$). Chlorophyll concentration ($mg\,m^{-3}$) is calculated from the natural fluorescence flux F_f and the incident irradiance according to the expression

$$\text{Chl}\,a = F_f/(a^*_{c(PAR)}\Phi_f E_{0(PAR)}) \quad \text{units: mg Chl a m}^{-3}, \tag{8}$$

where $a^*_{c(PAR)}$ is the chlorophyll specific absorption coefficient and Φ_f is the quantum yield of fluorescence. These values are treated as constants in the software of the PUV-500 with values of $0.04\,m^2\,mg^{-1}$ Chl a and 0.045 E fluorescence per μE absorbed, respectively. $E_{o(PAR)}$ is the scalar irradiance over PAR (400–700 nm). The radiometer PUV 500 determines downwelling cosine irradiance (2π sr), $E_{d(PAR)}$. However, there is very little difference between attenuation coefficient for scalar and cosine PAR (Chamberlin et al., 1990). In this paper, the measured values $a^*_{c(PAR)}$ during the cruise are introduced in the model, and thus $a^*_{c(PAR)}$ is not considered as a constant.

3. Results and discussion

3.1. Daily variation in UVR and PAR in the air during the cruise

Daily irradiance in the air at 305, 320, 380 nm and PAR during the FRUELA cruise (Fig. 2) showed large changes arising from variations in

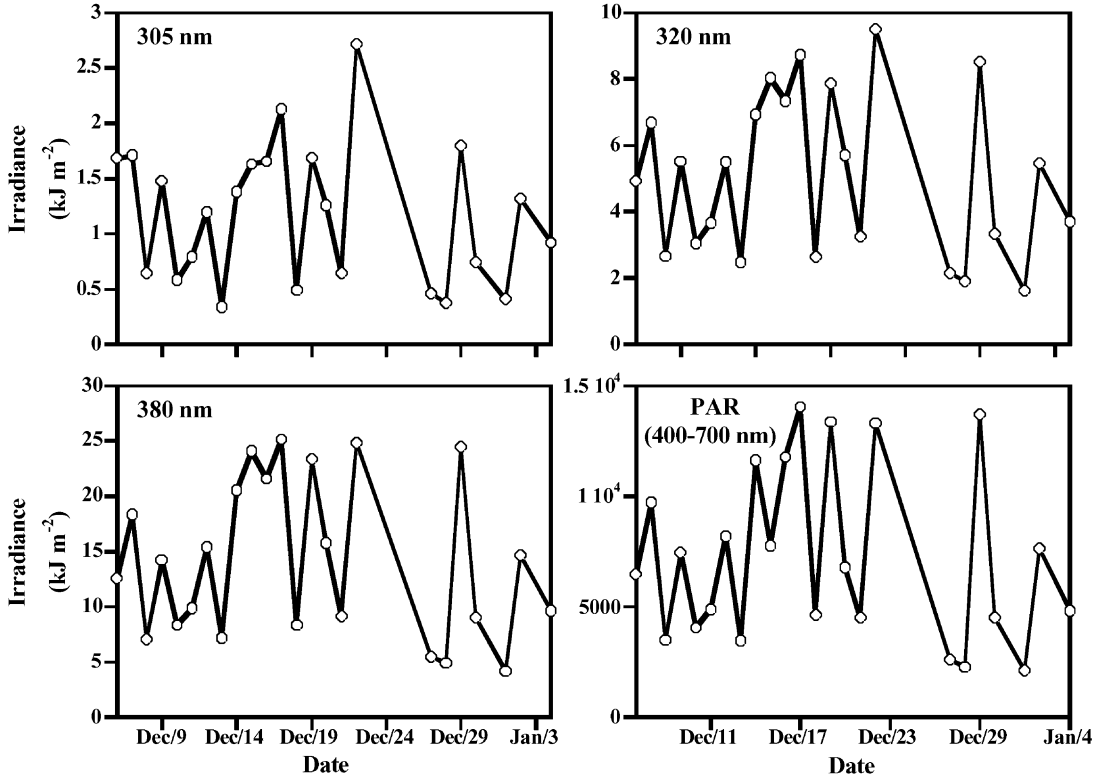

Fig. 2. Variations in the daily irradiance ($kJ\,m^{-2}$) at the surface during the FRUELA cruise at different UV wavelengths (305, 320 and 380 nm) and PAR (400–700 nm).

cloudiness. Another factor that affects the incident irradiance of UV-B radiation (280–315 nm) is the ozone concentration in the air. Although during the cruise ozone variations were not measured, large variations in this period are unlikely (Smith et al., 1992; Gautier et al., 1994). Thus the variations of surface UV-B can be attributed to the changes in cloud transmittance. In general, a good relation was found between the number of hours without clouds or with thin clouds and the daily UVR and PAR dose (data not shown). Gautier et al. (1994) showed that the Antarctica clouds have a profound effect on UV-B radiation, and their variations have a higher correlation with UV-B variations than ozone.

The daily variations at 380 nm wavelength and PAR showed a similar pattern, but this was different than those at 305 and 320 nm (Fig. 2). High values of 305/320 and 305/340 ratios were observed at the beginning of December. The increase in the 305/340 ratio has been used as an indicator of ozone depletion in the Earth's surface (Madronich et al., 1995; Stamnes et al., 1991). Thus during FRUELA cruise, a transient ozone hole was observed as indicated by the increase in 305/340 ratio (data not shown). Orce and Helbling (1997) found an ozone hole over Ushuaia (55°S, 68°W) for about 2 weeks during November–December 1995, at the same time as the FRUELA cruise.

The atmospheric noon values of irradiance at 305 nm showed great variations during the FRUELA cruise, ranging from $1.2\,\mu W\,cm^{-2}$ to a maximal value of $9.92\,\mu W\,cm^{-2}$, the average and standard deviation being $6.14\pm2.67\,\mu W\,cm^{-2}$, respectively. These maximal values are similar to those reported in different localities of Antarctic (for example Palmer station and Ushuaia) but were greater than those reported in McMurdo or the South Pole station (Weiler and Penhale, 1994; Booth et al., 1994, 1996). The last cited stations are integrated in the Polar Network for monitoring ultraviolet radiation supported by the US National Science foundation (Booth et al., 1994, 1996).

3.2. *Spatial variation in K_d and bea attenuation in Bransfield and Gerlache Straits*

In general the vertical attenuation coefficients of downwelling radiation for both UVR and PAR were higher in Gerlache than in Bransfield Strait waters (Table 1). High attenuation coefficients (c and K_d) in the UV range were also found in Bransfield close to a front occurring in this region. The front at about 61°S has previously been located in the North of Elephant and King George islands (Helbling et al., 1993). In this frontal system, the beam attenuation coefficient presented the highest values (0.8–0.9 m^{-1}) in Bransfield Strait

Table 1
Average values and standard deviation (±) of attenuation coefficient of the downwelling radiation at UV (305, 320, 340, 380 nm) and PAR (400–700 nm) in m^{-1} and beam attenuation coefficient (c, m^{-1}) in Bransfield and Gerlache Strait waters during the FRUELA 95 cruise[a]

Site	$K_{d(305)}$	$K_{d(320)}$	$K_{d(340)}$	$K_{d(380)}$	$K_{d(PAR)}$	c
Bransfield macroscale 4–9/12/95	0.332±0.120	0.373±0.170	0.334±0.170	0.223±0.011	0.185±0.070	1.334±0.130
Bransfield mesoscale 13–19/12/95	0.284±0.142	0.262±0.030	0.209±0.035	0.157±0.034	0.155±0.033	1.252±0.141
Gerlache 10–12/12/95	0.283±0.102	0.432±0.092	0.422±0.087	0.296±0.063	0.227±0.044	1.385±0.423
Gerlache daily cycles 20–21/12/95	0.312±0.161	0.462±0.071	0.393±0.072	0.293±0.052	0.219±0.022	1.152±0.123
Gerlache daily cycles 26–30/12/95	0.231±0.071	0.364±0.061	0.329±0.082	0.248±0.061	0.194±0.023	1.123±0.202
Gerlache daily cycles 1–3/1/96	0.278±0.162	0.465±0.103	0.469±0.201	0.369±0.22	0.316±0.043	1.731±0.401

[a] The data are presented according to the region analysed (Bransfield and Gerlache), to the different research phases of the FRUELA cruise (macroscale, mesoscale and daily cycles) and date.

waters (Helbling et al., 1993). In the FRUELA cruise, the frontal system was found at 62–63°S. In the inner region of Bransfield Strait, the penetration of UV and PAR was higher than on the border of Bransfield region. The beam attenuation coefficient presented the same pattern with higher values in the border than in the inner region of Bransfield (Table 1).

The maximal values of K_d and c were found in Gerlache waters (Table 1). $K_{d(PAR)}$ and $K_{d,(380)}$ values are in the range reported in Bellingshausen and Amundsen seas (Stambler et al., 1997), with the greatest values in Gerlache waters due to higher chlorophyll concentration in Gerlache than in Bellingshausen and Amundsen seas.

Good correlation between K_d at 320, 340 and 380 nm and chlorophyll concentration was found including all stations ($n = 98$; 320 ($r = 0.69$, $p < 0.01$), 340 nm ($r = 0.814$, $p < 0.01$), and 380 nm ($r = 0.84$, $p < 0.01$). Although chlorophyll does not present high absorption at 320, 340 and 380 nm, this correlation could be attributed to substances that covary with chlorophyll, such as mycosporine-like aminoacids within the phytoplankton absorbing in this range (Karentz et al., 1991; Karentz, 1994).

3.3. *Profiles of UV and PAR radiation in Gerlache and Bransfield Straits*

In order to illustrate the main differences in the UV-PAR penetration and water transmission in Bransfield and Gerlache region several profiles were selected (Figs. 3–4). Stations 15 and 94 had similar $K_{d(PAR)}$ values (0.279 and 0.210, respectively); however beam attenuation profiles were different (Fig. 5). This can be explained by the physical and biological structure of these two different water types. Station 15 is located in the front with a large mixed layer. The transmission in this station ranged between 62% and 65% from surface to 45 m depth, indicating a homogeneous distribution of particles. On the other hand, station 94 (63°57′S, 60°16′W), located on the coast of Trinity Peninsula south of Trinity Island, presented a stratified water column and the particles were distributed according to a density gradient with maximal concentration of particles (mainly cryptomonads cells) at surface waters (5–15 m depth). This is clearly observed in the transmission profile; for example, the minimal transmission (about 45%) corresponded to the maximum concentration of cells and maximum chlorophyll fluorescence (Fig. 3).

In contrast, station 123 is located in more transparent water than stations 15 and 94 (Fig. 3). The penetration of UV-B radiation is very high due to the large transmission in water (about 80% from 0 to 50 m depth). The physical structure of this station indicated the existence of well-mixed waters, similar to station 15, but contained a smaller amount of particles since station 15 is located in the front.

Station 140 (63°7′S, 59°25′W) was in another region of the Bransfiel Strait, with a high concentration of particles and consequently relatively high K_d values, similar to those found in the frontal system and in the coastal waters south of Trinity Island. The beam attenuation profiles indicated high concentration of particles about 10–20 m depth, corresponding to relatively stratified waters (Fig. 5). The phytoplankton maximum is located deeper, and the number of cells is lower than in stratified coastal waters. Such differences between stations can be clearly seen in the UV transmission. The 1% depth for UV radiation (305 nm) reaches about 20 m at stations 123 and 149 but only 10–15 m at stations 15 and 94. The 1% depth for PAR was 50–55 m in the stations with clear waters and 18–30 m in the stations with turbid waters.

Clear differences in the bio-optical characteristics were observed between the two extreme parts of Gerlache Strait: 64°S 62°W (station 47) and 65°S 64°W (station 156.3), compared to the central part, 64.5°S 62.5°W (stations 177.3, 184.4). In the entrance of the Strait (station 47), the UVR and PAR attenuations (Fig. 4) were very high, with $K_{d(PAR)}$ 0.274 m^{-1}. This value is similar to that described in the frontal system, but again it corresponded to a different hydrographic structure. Station 47 showed stratified waters with a very high concentration of particles (mainly cryptomonads) as shown by the very low transmission (about 50% between 0 and 10 m). Light penetration increased in the mid-region of

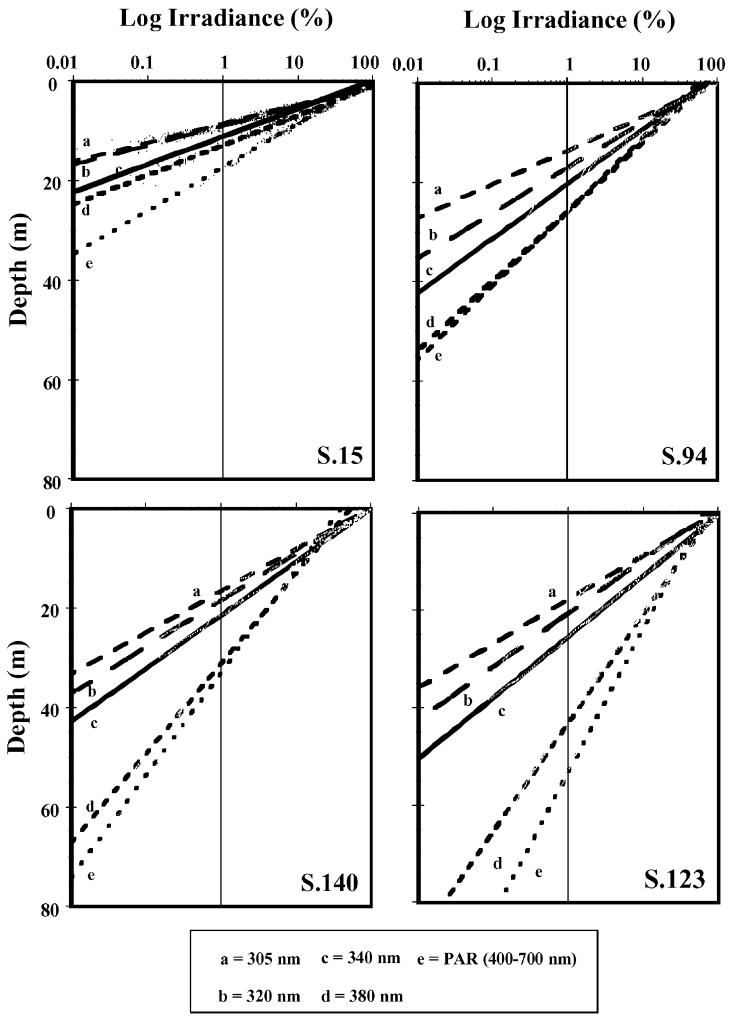

Fig. 3. Irradiance profiles (log irradiance) with depth at different stations of Bransfield region at four different UV wavelengths (305, 320, 340 and 380 nm) and PAR (400–700 nm). A vertical line indicates the depth at which 1% of surface radiation is reached ($D_{1\%}$)

Gerlache Strait compared to both extremes. In stations 177 and 184 the $K_{d(PAR)}$ was 0.156 and 0.195 m^{-1}, respectively (Fig. 4). The beam attenuation profile was more similar to that of the southern part than to that of the northern one (Fig. 6), with a transmission of 75% between 0 and 10 m, while 80–85% transmission was found in deeper waters (from 20 to 80 m depth). These differences were found in a relatively short-term period (several days). Particles concentration determined later (30 December 1995–4 January 1996) in the mid-region of Gerlache (stations 177, 178 and 184) decreased compared to station 47 (10 December 1995), indicating a relatively rapid horizontal water mass movement from the northern to the southern part of Gerlache Strait.

UV penetration was higher in Bransfield than in Gerlache Strait waters, and thus different effect of UV radiation on C fixation in these two regions was expected. UV irradiance at surface level was very high, mainly in early December and also during the first week of January. A depletion of C

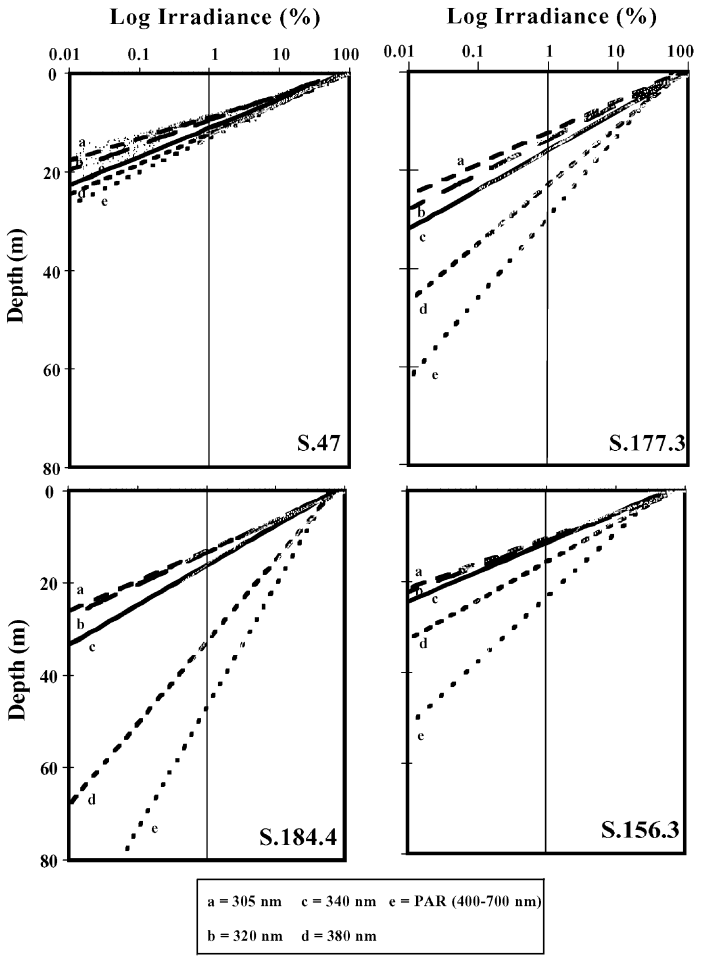

Fig. 4. Irradiance profiles (log irradiance) with the depth at different stations of Gerlache region at four different UV wavelengths (305, 320, 340 and 380 nm) and PAR (400–700 nm). the vertical line indicates $D_{1\%}$.

fixation by UV radiation is expected in this period of high UV penetration. Figueroa et al. (1997a) observed higher inhibition in the short-term of C-fixation by UV-A + UV-B (82%) than by UV-A (72%) in cryptomonads collected from Gerlache waters. On the other hand, the percentage of inhibition by artificial UV radiation of carbon fixation was inversely correlated with bio-optical characteristics as specific attenuation coefficient for PAR (K_d^*), percentage of water transmission and the dose of UV radiation received in the natural environment 24 h before sampling (Figueroa et al., unpublished). Cells (mainly cryptomonads) collected from Gerlache waters with high beam-attenuation coefficients and low chlorophyll specific-absorption coefficients showed higher inhibition of C fixation by artificial UV radiation than cells collected from Bransfield waters with a high microplankton/nanoplankton ratios, high water transparency, low beam-attenuation coefficients and high specific-absorption coeffients due to phytoplankton (Figueroa et al., unpublished).

3.4. *Underwater light spectra in Gerlache and Bransfield Straits*

In addition to the differences in K_d for UVR and PAR between Bransfield and Gerlache straits

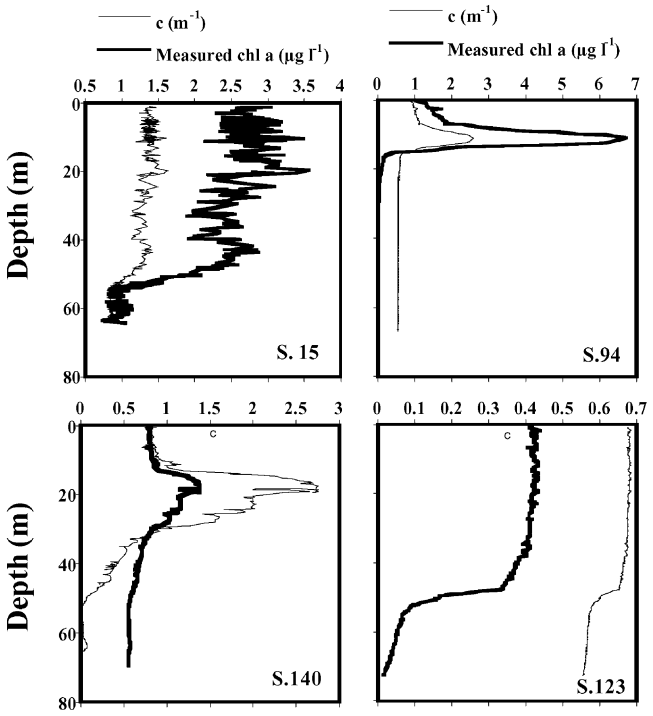

Fig. 5. Profiles of beam attenuation coefficient (m^{-1}) and chlorophyll concentration in different stations of Bransfield region calculated from the function between measured and estimated chlorophyll, according to the bio-optical model of Kiefer et al. (1989).

waters, variations in the spectral photon fluence rate for the whole spectrum (300–800 nm) were detected (Fig. 7). Thus, in station 29, located in the frontal system with $K_{d(PAR)} = 0.2772\,m^{-1}$, a light depletion between surface waters and 5 m depth is mainly produced in the far-red and red parts of the spectrum. However in Bransfield, south of Deception Island with clear waters (station 168 station, $K_{d(PAR)} = 0.152\,m^{-1}$), the high relative extinction in the blue and red parts of the spectrum occurred only below 20 m depth. Maximum light penetration is reached at 530 and 522 nm at 4 and 40 m, respectively. In the northern entrance of Gerlache Strait the extinction of red and blue light was very high (station 178, $K_{d(PAR)} = 0.282\,m^{-1}$); the maximum transmission was at 530 and 528 nm, at 4 and 40 m respectively. In the northern mid-Gerlache region (station 184, $K_{d(PAR)} = 0.389\,m^{-1}$), the pattern was similar to station 178 but with higher depletion of the blue region of the spectrum. Maximum transmission was at 556 and 536 nm, at 4 and 40 m, respectively. In the south (station 177, $K_{d(PAR)} = 0.156\,m^{-1}$), the waters became clearer than in the northern region (stations 178, 184) and southern entrance (station 169, $K_{d(PAR)} = 0.217\,m^{-1}$). Thus, station 177 showed a similar pattern to the Bransfield stations, with lower depletion of blue and red parts of the spectrum than in northern and southern stations. Finally, the depletion of red and blue was again high in station 169. The maximal transmission ocurred at 554 and 556 nm at 4 and 40 m in both 177 and 169 stations.

The higher depletion between 2 and 6 m in northern and southern stations of Gerlache Strait is explained by the very high density of phytoplankton in this water layer corresponding to the minimum transmission in the surface waters of these stations (between surface and 10 m). Although the number of particles was apparently similar through in the upper 10 m, the most drastic depletion occurred between 2 and 6 m depth. The

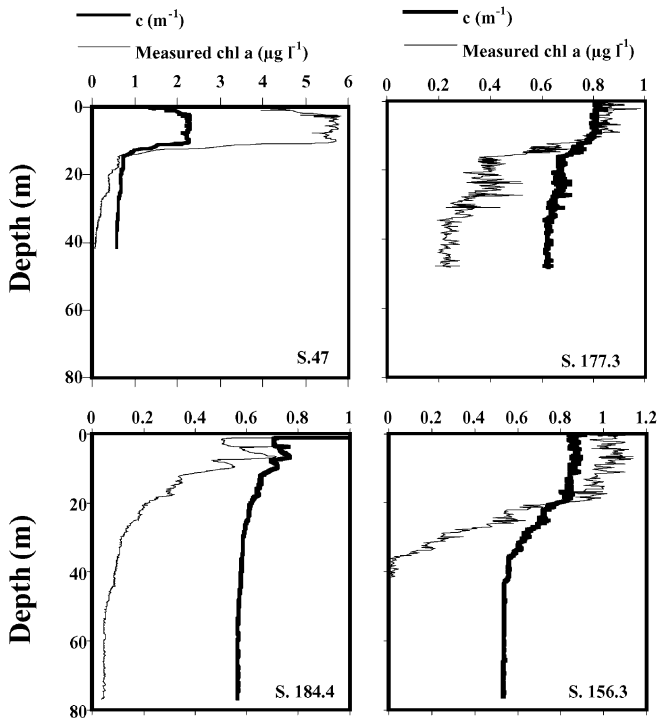

Fig. 6. Profiles of beam attenuation coefficient (m^{-1}) and chlorophyll concentration in different stations of Gerlache region calculated from the function between measured and estimated chlorophyll, according to the bio-optical model of Kiefer et al. (1989).

highest depletion in Bransfield and mid-Gerlache stations, with a lower amount of phytoplankton, was found between 10 and 20 m.

3.5. *Relation between chlorophyll deter ined fro the bio-optical odel reported by Kiefer et al. (1989) and chlorophyll easured in Gerlache and Bransfield Straits*

A good linear correlation ($r = 0.897$, $p < 0.05$, $n = 50$) was found between measured chlorophyll and estimated chlorophyll according to the bio-optical model of Kiefer et al. (1989). First, a constant value of $a^*_{c(PAR)}$ of 0.04 was used, but when the actual values were included according to Eq. (3), the correlation was improved. This bio-optical model was useful for the estimation of chlorophyll in the Gerlache and Bransfield region. One of the main practical uses of this calculation is to produce a quasi-continuous chlorophyll profile. The similarities between chlorophyll and beam attenuation profiles are very clear through the selected stations of Bransfield and Gerlache waters (Figs. 5–6). Light attenuation in this region is highly correlated with chlorophyll concentration ($p < 0.01$, $r = 0.95$). In Bransfield waters different profiles were found, those with low beam attenuation (station 15, c_{max} about $1.5\,m^{-1}$) in the front and those with high beam attenuation (station 94, c_{max} = about $4.5\,m^{-1}$) on the coast of Trinity Peninsula. The amount of total particles in the water column was not the only difference between coastal waters and the Bransfield Strait but also the distribution throughout the water column. Thus, the particles were more homogenously distributed in Bransfield Strait, whereas a very strong stratification was detected in Gerlache Strait and in the front of Bransfield. A linear correlation ($r = 0.62$, $p < 0.05$, $n = 94$) between

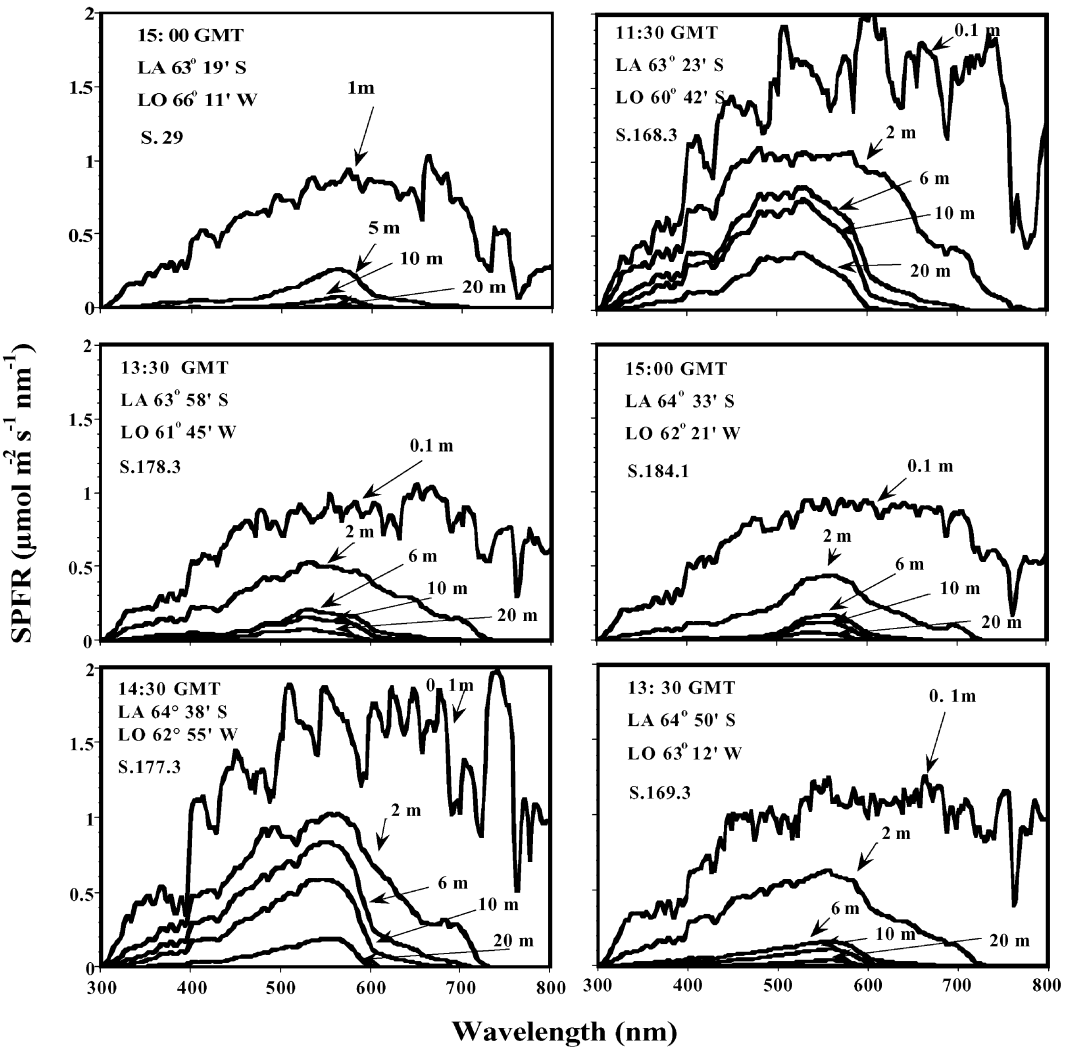

Fig. 7. Spectral photon fluence rate (SPFR) in $\mu mol\,m^{-2}\,s^{-1}\,nm^{-1}$ at different stations of Bransfield (29 and 168.3) and Gerlache (178.3, 184.3, 177.3 and 169.3) region in the surface (0.1 m) and at different depths.

beam attenuation coefficient and dissolved organic carbon also was found.

The concentration of chlorophyll is usually well correlated (correlation coefficient exceeding 0.7–0.8) with the beam attenuation coefficient (c) for $\lambda < 600\,nm$ in Case I waters (Mitchell and Holm-Hansen, 1991a). Case I waters have been defined as clear waters with chlorophyll between 0.08 and $1.5\,mg\,m^{-3}$ (Smith and Baker, 1978). In the FRUELA cruise, a good correlation between $c - c_w$ and chlorophyll concentration also was observed (Fig. 8). The slope of the correlation function was greater in Bransfield than in Gerlache waters. This indicates higher contribution of chlorophyll to the light attenuation in Bransfield than in Gerlache waters. The reason for this significant correlation is that beam attenuation coefficient is dominated by scattering through the visible spectrum. Sagan et al. (1995) reported that values of $c - c_w$ (660 nm) varied from 0.2

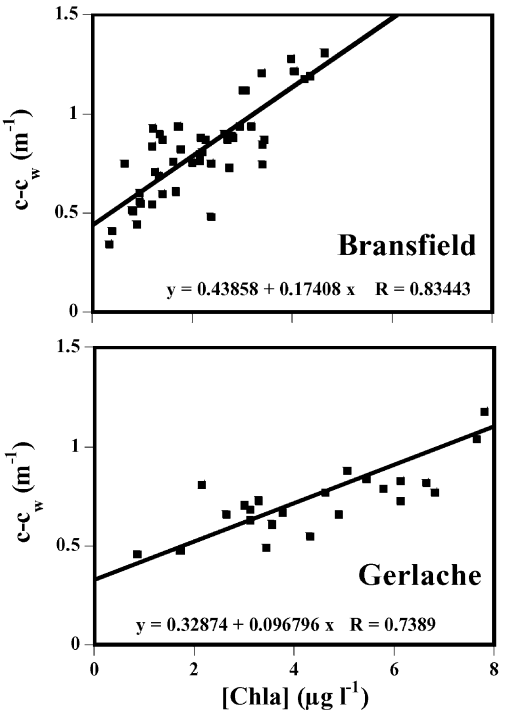

Fig. 8. Relationship between $c_t - c_w$, c_t being the total beam attenuation coefficient and c_w beam attenuation coefficient due to the water and chlorophyll concentration measured in all stations of Bransfield and Gerlache region.

to $1.2\,m^{-1}$ in Antarctic waters, generally being positively correlated with the chlorophyll concentration. The values of chlorophyll specific beam attenuation coefficient (c^*) in the part of the Bransfield area with low chlorophyll values ($<1\,mg\,m^{-3}$) were significantly greater than those usually found in Gerlache (data not shown). In Bransfield, c^* decreased with depth along with the chlorophyll specific absorption coefficient a^* (data not shown). This may be caused by the packaging effect in the large phytoplankton cells, or by acclimation to low light levels where the proportion of pigment per cell increases (Mitchell, 1992). Stramski and Reynolds (1994) reported higher c^* values during the day than at the night. In Bransfield waters, c^* increased with the depth in Gerlache, perhaps due to an increase in specific scattering coefficient (b^*) because of high concentration of particles in surface layers of the water column. In addition to the spatial variations reported in this study, Sagan et al. (1995) found temporal variations in c^* in the Bellingshausen Sea, i.e. lowest values during the night in the northern part of the sea and in the middle of the day in the southern part. This indicates a different pattern of particle distribution within the Bellingshausen Sea

In summary, during the FRUELA cruise three different regions were found with respect to bio-optical characteristics: (1) frontal system north of Bransfield, with $K_{d(PAR)} > 0.2\,m^{-1}$, c_{max} 1.5–$1.9\,m^{-1}$; (2) Bransfield region, with $K_{d(PAR)} < 0.1\,m^{-1}$ and c_{max} 0.9–$1.2\,m^{-1}$; and (3) Gerlache and coastal waters of Trinity Peninsula, with $K_{d(PAR)} = 0.18 - 0.545\,m^{-1}$ and c_{max} 1.5–$2.5\,m^{-1}$.

3.6. *Spectral attenuation coefficient ($K_{d,(\lambda)}$) and specific spectral attenuation coefficient ($K^*_{d,(\lambda)}$) in Gerlache Strait fro particulate aterial (k_p) and dissolved organic atter (k_s): relation to chlorophyll concentration and dissolved organic carbon*

The spectral attenuation coefficient was calculated in selected stations at Bransfield (station 41 and 168.3) and Gerlache (stations 178, 184, 177, 169). The minimum varied from 520 to 560 nm. A small peak was observed at 446 nm corresponding to the absorption of chlorophyll. Figueroa et al. (1997b) found a good exponential relationship between the slope of the function $K_{d,(\lambda)}$ versus wavelength range (400–575 nm) and chlorophyll concentration in the water column during a daily cycle. Figueroa et al. (1997b) suggested that this slope in the $K_{d,(\lambda)}$ spectra was a good indicator of the number and distribution of particles in the water column.

In order to compare the FRUELA bio-optic data with those of RACERs, specific attenuation coefficient spectra were calculated at the same wavelengths reported by Mitchell and Holm-Hansen (1991a) i.e. 410, 441, 488, 520, 560, 633 and 683 nm (Table 2, Fig. 9) and also at UV radiation wavelengths: 305, 320, 340 and 380 nm The differences are less in the green-yellow region of the spectrum (520–600 nm). Spectral values of $K^*_{d,(\lambda)}$, K_w and K_s are presented in Table 2. A good correlation was found between K_d and chlorophyll

Table 2
Spectral light attenuation parameters calculated from the RACER model proposed by Mitchell and Holm-Hansen (1991a)[a]

Wavelength (nm)	K^*_d	$(K_s + K_w)$	K_s	K_w [b]	K_w [c]	r^2	n
Bransfield							
305	0.025	0.116				0.03	45
320	0.059	0.107				0.70	49
340	0.032	0.135				0.64	51
380	0.029	0.080	0.040	0.040		0.72	57
PAR (400–700)*	0.023	0.069	0.006	0.063[d]		0.80	59
Gerlache							
305	0.034	0.014				0.92	9
330	0.030	0.167				0.83	9
350	0.031	0.074	0.051	0.023		0.87	14
410	0.025	0.061	0.036	0.025	0.022	0.77	16
440	0.030	0.053	0.031	0.022	0.017	0.84	17
488	0.017	0.115	0.090	0.025[e]	0.021	0.83	15
520	0.013	0.078	0.030	0.048	0.049	0.82	15
560	0.008	0.094	0.023	0.071	0.072	0.75	16
630	0.021	0.173	0	0.277	0.323[f]	0.66	13
680	0.035	0.185	0	0.510	0.470[g]	0.86	12
700	0.005	0.459	0	0.630		0.22	10

[a] K^*_d is the slope between specific diffuse attenuation coefficient (K_d) vs. Chl *a* concentration. K_w is the attenuation coefficient for pure water taken from Smith and Baker (1978) and Morel (1988), and K_s the attenuation due to soluble materials.
[b] Values from Smith and Baker (1978).
[c] Values from Morel (1988).
[d] Values represent the mid-wavelength of the interval between 400 and 700 nm (550 nm).
[e] Value approximated to 490 nm in Smith and Baker's table.
[f] Values from 633 nm in Morel's table.
[g] Values from 683 nm in Morel's table.

concentration at the different wavelengths analyzed: 410 nm ($r = 0.77$), 440 nm ($r = 0.84$), 488 nm ($r = 0.83$), 520 nm (0.83), 560 ($r = 0.76$) and 680 nm ($r = 0.86$). The highest correlations between chlorophyll and K_d were found in the blue wavelengths, agreeing with previous measurements in Antarctic waters (Mitchell and Holm-Hansen, 1991a; Stambler et al., 1997); but in contrast to the above cited papers, there was also a good correlation in red and green wavelengths. The high correlation between chlorophyll and K_d in green wavelengths in Gerlache is explained by the high relative proportion of cryptomonads, which absorb in the green region due to the presence of phycoerythrin.

On the other hand, a good correlation was also found between $K_{d,(\lambda)}$ and chlorophyll concentration (Table 2) at the different UV wavelengths analyzed: 320 nm ($r = 0.70$), 340 nm (0.69), 380 nm (0.72) and PAR ($r = 0.80$). At 305 nm no correlation was found. Maximal values of $K^*_{d,(\lambda)}$, were reached at 320 nm. $K^*_{d,(\lambda)}$, values at 340 nm were lower than those reported by Stambler et al. (1997) in Antarctic waters.

The FRUELA bio-optic data (Fig. 9) were plotted together with (a) the RACER data set ((Mitchell and Holm-Hansen, 1991a, b) the results of Smith and Baker (1978) for euphotic waters (Chl *a* + phaeopigments > 1.0 mg m^{-3}), (c) the predictions of Morel's model for 3.0 mg Chl *a* m^{-3} (the mean pigment concentration during RACER) and (d) the plot reported by Stambler et al. (1997). The spectra of the FRUELA cruise shows similarity to the RACER data but with higher specific attenuation in the whole spectrum from 400 to 700 nm. In addition to PAR, specific attenuation coefficient for UV is also shown. The $K^*_{d,(\lambda)}$, increased compared to blue region of the spectra. FRUELA data (as in RACER) showed clear differences from the models of Smith and

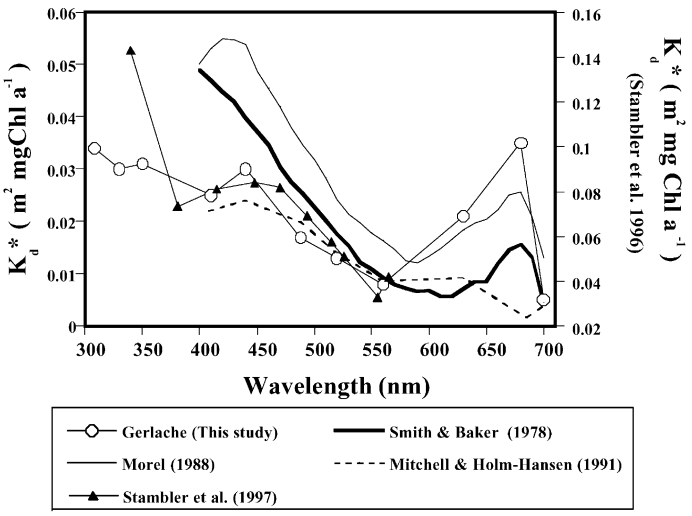

Fig. 9. (a) Specific spectral attenuation coefficient (K_d^*) in $m^2\,mg^{-1}$ Chl *a* in Bransfield and Gerlache region. K_d^* is calculated from the values at 305, 320, 340, 380 nm and PAR (400–700 nm). The values of PAR are represented at 400 nm for convenience. (b) K_d^* spectra of Gerlache region calculated at 305, 330, 350, 410, 440, 488, 520, 560, 630, 680 and 700 nm according to the model of Smith and Baker (1978). For comparison the K_d^* from RACER (Mitchell and Holm-Hansen, 1991a, b) and Bellinghausen region (Stambler et al., 1997) is included. The spectrum of Smith and Baker (1978) is from their model for euphotic waters (Chl *a* + phaeopigments > 1.0 mg m^{-3}) and the spectrum of Morel (1988) is a solution of the non-linear model corresponding to a pigment concentration equivalent to the mean values observed during RACER (Chl *a* + phaeopigments = 3.0 mg m^{-3}).

Baker (1978) and Morel (1988). In particular, the values of $K_{d,(\lambda)}^*$, in the blue region (400–500 nm) are about 30–40% lower than those of the previous data sets for mid-latitude and are significantly different ($p < 0.05$).

In Gerlache waters both K_d^* values at green and red wavelengths (Table 2) were substantially higher than in previous data from Antarctica Peninsula waters (Mitchell and Holm-Hansen, 1991a) but much lower than those reported in the Admudsen and Bellingshausen seas (Stambler et al., 1997). This can be explained because of different phytoplankton populations and chlorophyll values in the different studies in Gerlache compared to Admundsen and Bellingshausen Seas. The K_d^* values for PAR in Gerlache and Bransfield are in the range of those previously reported for Antarctic waters as for example 0.042 m^{-1} in the Northern Weddell Sea (Tilzer et al., 1994) and 0.068 m^{-1} in Admundsen and Bellinghausen seas (Stambler et al., 1997). The Antarctic K_d^* values for PAR are generally higher than those in other water types (Kirk, 1994). This may be due to the minimal self-shading of the algae by the sparse phytoplankton in the Antartctic waters.

Acknowledgements

This work was financed by the CYCYT project (Spain) ANT94-1010. The author thanks Ivan Gómez, Eduardo Pérez and Ingrid Palica for data processing and discussion of the results, the crew of the B.I.O. Hespérides, and all our colleagues during the FRUELA-95 cruise for their help and cooperation.

References

Behrenfeld, M.J., Lean, D.R.S., Lee II, H., 1995. Ultraviolet-B radiation effects on inorganic nitrogen uptake by natural assemblages of oceanic plankton. Journal of Phycology 31, 25–36.

Booth, C.R, Lucas, T.B., Morrow, J.H., Weiler, C.S., Penhale, P.A., 1994. The United States National Science Foundation's polar network for monitoring ultraviolet radiation.

In: Weiler, C.S, Penhale, P.A. (Eds.), Ultraviolet Radiation in Antarctica: Measurements and Biological Effects. Antarctic Reseach Series 62, 17–37.

Booth, C.R., Lucas, T.B, Metechkina, T, Tusson, J.R., Smith, J.O., Neuschuler, D.A., Morrow, J.H. 1996. NSF Polar Programs UV spectroradiometer Network 1994–1995 operations report. Biospherical Instrument Inc., 182 pp.

Chamberlin, W.S., Booth, C.R., Kiefer, D.A., Morrow, J.H., Murphy, R.C., 1990. Evidence for simple relationship between natural fluorescence, photosynthesis, and chlorophyll in the sea. Deep-Sea Research 37 (6), 951–973.

Clarke, A., 1988. Seasonality in the Antarctic marine environment. Comparative Biochemistry and Physiology 90, 461–473.

Figueiras, F.G., Pérez, F.F., Pazos, Y., Ríos, A.F., 1994. Light and productivity of Antarctic phytoplankton during austral summer in an ice edge region in the Weddell–Scotia Sea. Journal of Plankton Research 16, 233–235.

Figueroa, F.L., Blanco, J.M., Jiménez-Gómez, F., Rodríguez, J., 1997a. Effects of ultraviolet radiation on carbon fixation in Antarctic nanophytoflagellates. Photochemistry and Photobiology 66, 185–189.

Figueroa, F.L., Ruiz, R., Sáez, E., Lucena, J., Niell, F.X., 1997b. Spectral light attenuation and phytoplankton distribution during a daily cycle in the reservoir of La Concepción, Southern Spain. Archiv für Hydrobiologie 140, 71–90.

Gautier, C., He, G., Yang, S., Lubin, D., 1994. Role of clouds and ozone on spectral ultraviolet-B radiation and biologically active UV dose over Antarctica. In: Weiler, C.S., Penhale, P.A. (Eds.), Ultraviolet Radiation in Antarctica: Measurements and Biological Effects. Antarctic Research Series 62, 83–91.

Häder, D.-P., 1994. UV-B effects on aquatic ecosystems. In: Hilton, R., Joyner, E.B. (Eds.), UV-B Radiation in the Biosphere Stratospheric Ozone Depletion. Springer, Heidelberg, pp. 155–161.

Helbling, E.W., Amos, A.F., Silva, N.S., Villafañe, V., Holm-Hansen, O., 1993. Phytoplankton distribution and abundance as related to a frontal system north of Elephant Island, Antarctica. Antarctic Science 5, 25–36.

Helbling, E.W., Villafañe, V., Holm-Hansen, O., 1994. Effects of ultraviolet radiation on Antarctic marine phytoplankton photosynthesis with particular attention to the influence of mixing. In: Weiler, C.S., Penhale, P.A. (Eds.), Ultraviolet Radiation in Antarctica: Measurements and Biological Effects. Antarctic Research Series 62, 207–227

Holm-Hansen, O., Mitchell, B.G., 1991. Spatial and temporal distribution of phytoplankton and primary production in the western Bransfield Strait region. Deep-Sea Research II 38, 961–980.

Holm-Hansen, O., Helbling, E.W., Lubin, D., 1993a. Ultraviolet radiation in the Antartica: inhibition of primary production. Photochemistry and Photobiology 58, 567–570.

Holm-Hansen, O., Lubin, D., Helbling, E.W., 1993b. Ultraviolet radiation and its effects on organisms in aquatic environments. In: Young, A.R. (Ed.), Enviromental UV Photobiology. Plenum Press, New York, pp. 379–425.

Huntley, M., Karl, D.M., Niler, P., Holm-Hansen, O., 1991. Research on Antarctic coastal ecosystem rates (RACER): an interdisciplinary field experiment. Deep-Sea Research II 38, 911–941.

Jerlov, N.G., 1976. Marine Optics. Elsevier, Amsterdam.

Karentz, D., 1994. Ultraviolet tolerance mechanisms in Antarctic marine organisms. In: Weiler, C.S., Penhale, P.A. (Eds.), Ultraviolet Radiation in Antarctica: Measurements and Biological Effects. Antarctic Research Series 62, 93–110.

Karentz, D.J., Mceuen, E.S., Land, M.C., Dunlap, W.C., 1991. Survey of mycosporyne-like amino acid compounds in Antarctic marine organisms: potential protection from ultraviolet exposure. Marine Biology 108, 157–166.

Karl, D.M., Tilbrook, B.D., Tien, G., 1991. Seasonal coupling of organic matter production and particle flux in the western Bransfield Strait, Antarctica. Deep Sea Research II 38, 1097–1126.

Kiefer, D.A., Chamberlin, W.S., Booth, C.R., 1989. Natural fluorescence of chlorophyll *a*: relationship to photosynthesis and chlorophyll concentration in the Western South Pacific gyre. Limnology and Oceanography 34, 868–881.

Kirk, J.T.O., 1994. Light and Photosynthesis in Aquatic Ecosystems, 2nd Edition. Cambridge University Press, Cambridge, p 509.

Kishino, M., Takahashi, N., Okami, N., Ichimura, S., 1985. Estimation of the spectral absorption coefficients of phytoplankton in the sea. Bulletin of Marine Science 37, 634–642.

Lesser, M.P., Cullen, J.J., Neale, P.J., 1994. Carbon uptake in a marine diatom during acute exposure to ultraviolet B radiation: relative importance of damage and repair. Journal of Phycology 30, 183–192.

Lewis, M.R., Warnock, R.E, Platt, T., 1985. Absorption and photosynthetic action spectra for natural phytoplankton populations: implications for production in the Open Ocean. Limnology and Oceanography 30 (4), 794–806.

Madronich, S., Mackenzie, R.L., Caldwell, M.M., Björn, L.O., 1995. Changes in ultraviolet radiation reaching the earth's surface. Ambio 24 (3), 143–152.

Mitchell, B.G., 1992. Predictive bio-optical relationships for polar oceans and marginal ice zones. Journal of Marine Systems 3, 91–105.

Mitchell, B.G., Holm-Hansen, O., 1991a. Bio-optical properties of Antarctica peninsula waters: differentiation from temperature ocean models. Deep-Sea Research II 38, 1009–1028.

Mitchell, B.G., Holm-Hansen, O., 1991b. Observations and modelling of the Antarctic phytoplankton crop in relation to mixing depth. Deep-Sea Research II 38, 981–1007.

Morel, A., 1988. Optical modelling of the upper ocean in relation to its biogeneous matter content (case I waters). Journal of Geophysical Research 93, 10749–10768.

Orce, V.L., Helbling, E.W., 1997. Latitudinal UVR-PAR measurements in Argentina: extent of the "ozone hole". Global and Planetary change 15, 113–121.

Prézelin, M.M., Boucher, N.P., Smith, R.C., 1994. Marine primary production under the influence of Antartic ozone

hole: Icecolors 90In:. In: Weiler, C.S., Penhale, P.A. (Eds.), Ultraviolet Radiation in Antarctica: Measurements and Biological Effects, Antarctic Research Series. American Geophysical Union, Washinghton, DC, pp. 159–186.

Sagan, S., Weeks, A.E., Robinson, I.S., Moore, G.F., Aiken, J., 1995. The relationship between beam attenuation coefficient and chlorophyll concentration and reflectance in Antarctic watres. Deep-Sea Research II 42, 983–996.

Schofield, O., Kronn, B.M.A., Prézelin, B.B., 1995. Impact of UV-B radiation on photosystem II activity and its relationship to the inhibition of carbon fixation rates for Antarctic ice algae communities. Jounal of Phycology 31, 703–715.

Smith, R.C., Baker, K.S., 1978. The bio-optical state of the ocean waters and remote sensing. Limnology and Oceanography. 23, 247–259.

Smith, R.C., Prézelin, B.B., Bidigare, R.R., Baker, K.S., 1989. Bio-optical modelling of photosynthetic production in coastal waters. Limnology and Oceanography 34, 1524–1544.

Smith, R.C., Prézelin, B.B., Baker, K.S., Bidigare, R.R., Boucher, N.P., Coley, T., Karentz, D., Macintyre, S., Maltick, H.A., Menzeis, D., Ondrusek, M., Wan, Z., Waters, K.J., 1992. Ozone depletion: ultraviolet radiation and phytoplankton biology in Antarctic waters. Science 225, 952–959.

Sosik, H.M., 1996. Bio-optical modelling of primary production: consequences of variability in quantum yield and specific absorption. Marine Ecology Progress Series 143, 225–238.

Stambler, N., Lovengreen, C., Tilzer, M.N., 1997. The underwater light field in the Bellinghausen and Admudsen Seas (Antarctica). Hydrobiologia 344, 41–56.

Stamnes, K.J., Slusser, R., Bowen, M., 1991. Derivation of total ozone abundance and cloud effects from spectral irradiance measurements. Applied Optics 30, 4418–4426.

Stramski, D., Reynolds, R.A., 1994. Diel variations in the optical properties of marine diatoms. Limnology and Oceanography 38, 1347–1364.

Tilzer, M.M., Dubinsky, Z., 1987. Effects of temperature and daylength on the mass balance of Antarctic phytoplankton. Polar Biology 7, 35–42.

Tilzer, M.M., Gieskes, W.W., Heusel, R., Fenton, N., 1994. The impact of phytoplankton on spectral water transparency in the southern ocean: implications for primary productivity. Polar Biology 14, 127–136.

Vernet, M., Brody, E.A., Holm-Hansen, O., Mitchell, G., 1994. The response of Antarctic phytoplankton to ultraviolet radiation: absorption, photosynthesis, and taxonomic composition. Antarctic Research Series 62, 143–158.

Weiler, S.C., Penhale, P.A., 1994. Ultraviolet Radiation in Antarctica: Measurements and Biological Effects. American Geophysical Union, Washington, DC.